Chapter 3

Fractography on Rigid Ceramics with Ultra-High-Molecular-Weight Polyethylene Fabric after Ballistic Impacts

Giovanni Barrera Torres, Juan Manuel Vélez and
Carlos Mario Gutierrez

Additional information is available at the end of the chapter

http://dx.doi.org/10.5772/63576

Abstract

The impact protection systems have traditionally been developed with metallic materials and structural protection applied in the automotive sector; while personal protection systems and composite systems evolve very fast, these systems have a large increase in applications due mainly to the amplitude of the manufacturing process. In the composite system for impact protection, it exposes both functionality and the rigid systems, aimed at structural protection, and flexible systems for personal protection. Nowadays, the development of materials with ballistic applications has emphasized protection of lightweight materials, for protection against projectiles of high and low speeds, among which are the bullets from weapons, fragments of tempered steel grenade hand or aircraft fragments, or a vehicle at high speed directly against housing and human integrity. It is necessary to investigate the mechanisms of fracture of the materials usually used for protection against impact, thus, it is possible to obtain important design systems that reduce the probability of failure and protect human lives and reduce damage to infrastructure information. In this chapter, the behavior of laminate sandwich-type systems, made from handcrafted ceramic plates with sheets of polyethylene (**ultra-high-molecular-weight polyethylene**, UHWMPE) against the impact of a metallic projectile, has been explored. The experimental work was made of two groups with different arrangements: the first group with the side that receives the impact of ceramic material (silicon carbide, SiC)-backed polymeric material and the second group with the side that receives the impact on polymer-backed ceramic material, the plates had dimensions 200 mm^2 of thickness to 5 mm for single plates and 20 mm for double plates. The experimental test was performed following the parameters of impact of NIJ III A standard. Some mechanisms (morphologies) of dissipation of kinetic energy received in the components were identified, as cited below, first in the ceramic material the formation of a crater, fracture, and delamination was observed, formed in the double and simple plates. Later, in the fabric polymeric material deformation mechanisms, such as the origination of defibrillation, conical geometry formation, delamination, twisting, and melting fibers due to the tribological contact of the metal shell impact, were observed. The exploration was culminated making a comparison between the arrangement that had higher energy absorption compared to an additional system designed with a ceramic (SiC) with less porosity, also aside to this chapter, it shows some of the deformed projectiles with a basic description of the fracture obtained after the impact, complementing the overall analysis of the systems used.

Keywords: ballistic impact, UHWMPE, SiC, fractography, delamination

1. Introduction

Currently, the need to use protection systems has increased sudden impacts that may cause damage to human or structural integrity, for example, the fall of a hammer, splashing chip result of the fall or 1indirect impact of a solid on a tornado, and the possibility of metallic projectile impact, in military use. In industry, some of the energy dissipation mechanisms and phenomena that accompany projectile impact environment-specific materials are still unknown. In order to advance the development of materials or focus on the protection of these eventual systems, it is important to take steps to identify environmental problems, to advance the possibility of effective impact protection solutions using known materials, using research like this, but with effective collaboration to develop solutions and further reducing noise by lack of resources. It is necessary to obtain collaboration of several entities, such as state and university-industry scientific and further technological development. The research on ballistic protection has restricted nature; due to the qualification of the subject as strategic, it is necessary to continue in these strategic research for the preservation of life, and the use of high-tech materials, call the research the development of materials that have a minimal negative impact on the environment, which would be a second function of protecting life.

2. Protection systems

A protection system emerges as an assembly of components where each has its own functions to protect an item or human being through the absorption of kinetic energy derived from direct or indirect collision with a projectile. Systems can be flexible, formed by rigid or polymer fabrics or metals, or ceramic plates and rigid polymers. Systems can be formed by various materials as sandwich panels; an example applied is usually illustrated in **Figure 1**. The penetration mechanism is shown in a system designed by a combination of plastic, center of ceramic material, with a backrest-purpose flexible application–specific protection material.

The polymers have been occupying spaces where metal and ceramic materials were predominant, now in response to the need for mass reduction, polymeric materials have applications in light protection such as suits, military [1] hardware, and rigid applications in specific parts of helicopters and land vehicles. Compounds systems aim at combining the properties of individual resistance of each material to obtain a higher property required. In recent years, with the ultrahigh molecular weight polyethylene (**UHWMPE**) sheet and addressing, different fibers get increased kinetic energy absorption [2]. The composite systems may be obtained in a variety of ways with advanced manufacturing processes [3]; with the fibers such as aramid and ultrahigh molecular weight polyethylene, it is possible to develop products for protection against projectiles, whereas ceramic materials without compromising the volume thereof do not represent effective protection and need to be combined with metal and/or polymers for designs in areas such as aerospace or personal protective competing with kinetic energy absorption of steel [4].

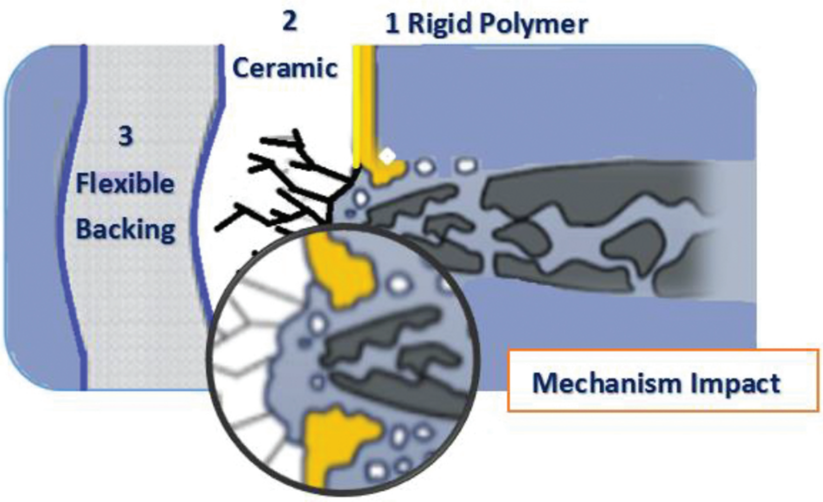

Figure 1. Composite panel (1, polymer; 2, ceramic flexible; 3, backing).

3. Materials and methods

The selection of materials was made from knowledge of the properties of polymers and ceramics used in ballistic applications [5–8]. Silicon carbide (SiC) was selected as the ceramic material because of the high hardness, high abrasion resistance, and its history in ballistic applications [9], besides being a commercial ceramic. The properties of SiC are due to the type of atomic bonding and crystalline structure hexagonal designed that cubic form α– SiC, the structure obtained depend on the method used for their production; in this case, the powder of silicon carbide used is produced by the Acheson process, which involves the reduction of silica sand in contact with petroleum coke or anthracite to a temperature close to 2400°C for 36 h, to form the commercial grade SiC α [10]. The properties of the ceramic used are as follows:

- Grain size: 10–50 μm
- Purity of material: silicon 80%, 20% silica binder based on cellulose apparent porosity of 40%

- Average true density: 1.60 g/cm³, obtained by making direct mass and volume of samples
- Temperature: 1250°C
- Plate dimensions: 197 ± 197 ± 3 mm × 3 mm × 5 ± 1 mm
- Average mass of plate: 293.4–312.9 g
- Theoretical density of SiC: 3.1–3.2 g/cm³ [11]
- Color: green
- Composed of compaction at atmospheric pressure, subsequently sintered in an electric furnace at 850°C

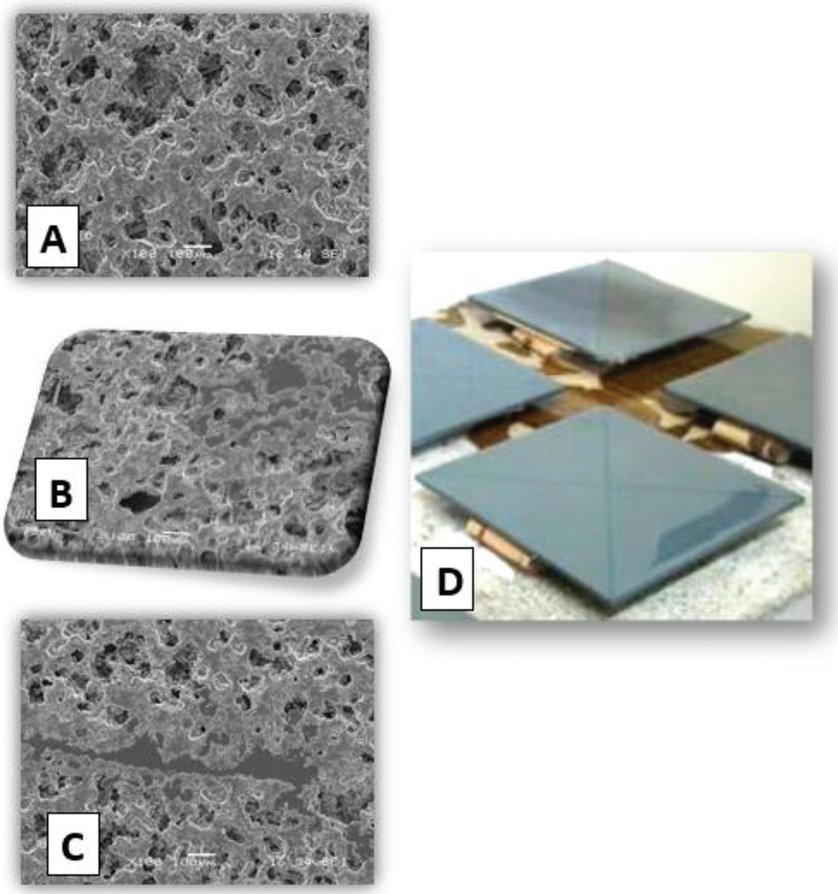

Figure 2. Morphology of the ceramic plates.

To determine the porosity of the samples, initially the specimens were dried and sintered in an oven at 850°C, then these were tested according to the ASTM C1039 standard for the apparent porosity of 40%; the surface porosity of the plates was 46% obtained using image analysis software. Image A in **Figure 2**, the plate obtained is shown unmodified, exhibits the surface porosity resulting from compaction process. Image B is observed at the surface of the plate with epoxy resin coating after dipping process, the isometric view. In image C, a portion

http://dx.doi.org/10.5772/63576

of the plate with magnification 100× microscopy, where the resin has achieved infiltration into the porous body thereof, image D, as can be seen to the shaped plate bodies, is observed to be adhered to the polyethylene sheet (UHWMPE).

The flexible material selected for the system embodiment was laminated fabric of ultrahigh molecular weight polyethylene (UHMWPE) given the properties of high kinetic energy absorption in ballistic protection systems published in the current literature. In **Figure 3**, the morphological composition of the panel, in which each of the layers consisting of parallel threads, in the configuration of two successive layers in the same orientation panel is observed; the next two layers are oriented perpendicularly to the direction of previous threads. In **Figure 3**, image A, the panel is illustrated with an impact recording, seen isometrically. In images B and C, the panel approach is illustrated; it is evident that the diameter of each wire was about 18 μm and the size of the fabric to the development of the system was 200 mm × 200 mm ±3.

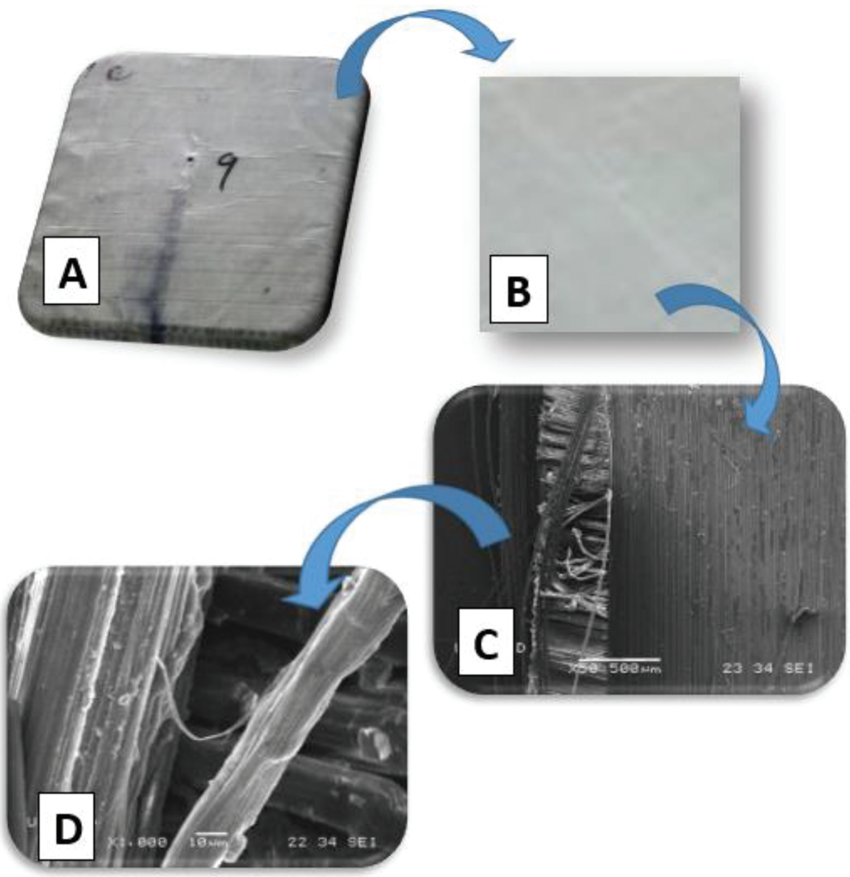

Figure 3. Images polyethylene ultrahigh molecular weight used.

The adhesive used in exploration is epoxy resin due to its good response, good heat sink residual stress, and compression stress [12], with better properties than polyester or phenolic resins have high hardness and very good adhesion in inhomogeneous materials [13]. Some of the properties of the epoxy resin used in this work are as follows:

Density: 1.1–1.4 g/cm^3.

Glass transition temperature: 120–190°C.

Viscosity: 113 centipoise at 22°C, viscosity taken in laboratory viscometer Brookfield of the Instituto Tecnológico Metropolitano, Medellin, Colombia. Main features are as follows: low shrinkage, good mechanical performance up to 180°C, good chemical resistance, high wear resistance, and high crack resistance.

3.1. Ballistic essays

As a destructive testing protocol, Ballistic Resistance of Body Armor NIJ Standard-0101.06, Section 4.2.1.2 [14], where the configuration of ballistics test is conditioned, is considered. In **Figure 4**, the graphical representation of the assembly for performing the impact test is observed. In **Figure 5**, the projectile used is shown, in side view, according to the standard for conducting the tests.

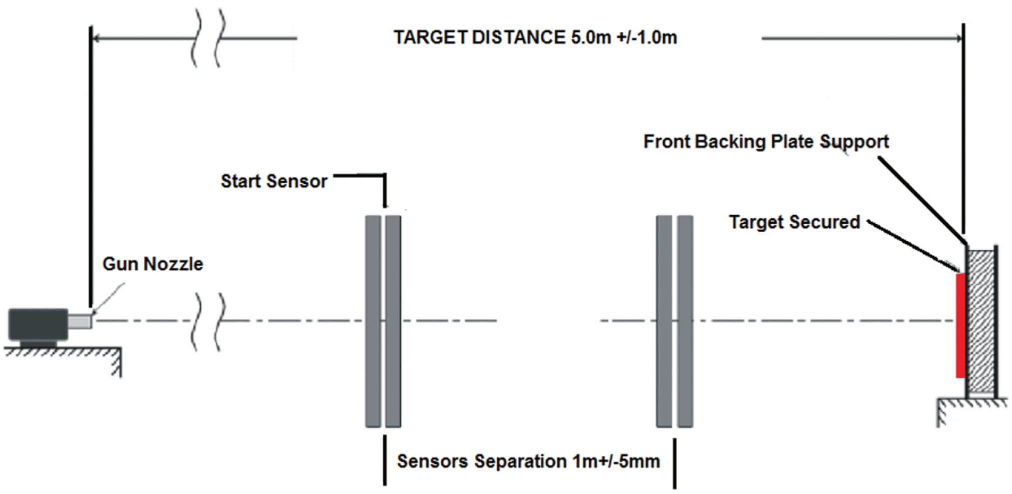

Figure 4. Assembly required for testing ballistic impact, NIJ standard.

Figure 5. Longitudinal dimensioning of the projectile used.

3.2. Fractography

For the characterization of the mechanism fault at macrometric scale, a calliper gauge to measure the diameters of the input crater and the output crater cone formed in the flexible phase of the system was used. To observe the cross section of a system, hydrocutting was used and the impact zone was analyzed, and to observe the details in the deformations through optical microscopy, the results are presented in the following sequence.

To manufacture the laminated composite systems the following process was carried out: they were placed, plates and sheets organized by polyethylene, in a cubic container that contains enough volume to be immersed in the epoxy resin, which was poured manually. The curing process of the resin is carried out at a room temperature of 19–25°C with a time period of 24 h because there it was recommended to use furnace having ceramic covered surface plates with epoxy resin; and the process contraction of the resin may crack the plates.

As a response variables to the impact factors such as diameters generated (input, output, and plastic cone on flexible material) are considered. In **Figure 6**, designs for impact analysis are shown. Group A (see from right to left) corresponds to the arrangement of the system with main layer receiving the projectile in woven polyethylene with ceramic backing and group B (see from left to right) corresponds to the arrangement of the system with main layer receiving the projectile in ceramic-backed polymer fabric. To perform the ballistic test for each impact system and perform characterization using optical microscopy, the samples were selected randomly to observe the predominant interaction in each of the systems.

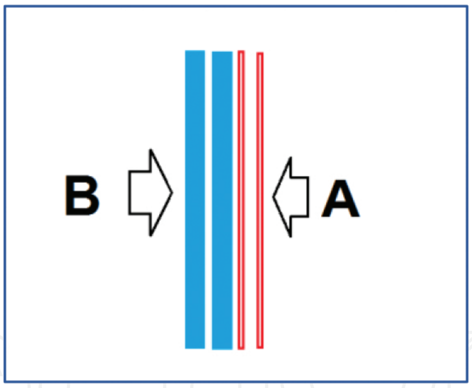

Figure 6. Impact sides. Direction side A: impact through UHWMPE; direction side B: impact through ceramics.

4. Results and discussions

4.1. Case I. Ceramic plate in front and polyethylene flexible as backing

In this case, the experiment was carried out placing the ceramic plate and receiving the metal projectiles, which were obtained with different morphology of some fractures as cited below. The bullet entered forming a crater that eroded an area of ≈3 mm around the crater and it is recalled that the initial diameter of the projectile was 9 mm. In **Figure 7**, drilling obtained as a result of the impact is illustrated in the left panel, the image formation of five cracks with perpendicular impact is illustrated in the right image; such fractures that move only by the surface plate without presenting complete rupture were observed. Possibly the presented erosion was due to the deformation process of the projectile, whereas the drilling system was due to their characteristics that greater drag is not imposed as a result if a large number of traces are drilled. The highlighted panel is uniform along the axial symmetrical quasierosion drilling.

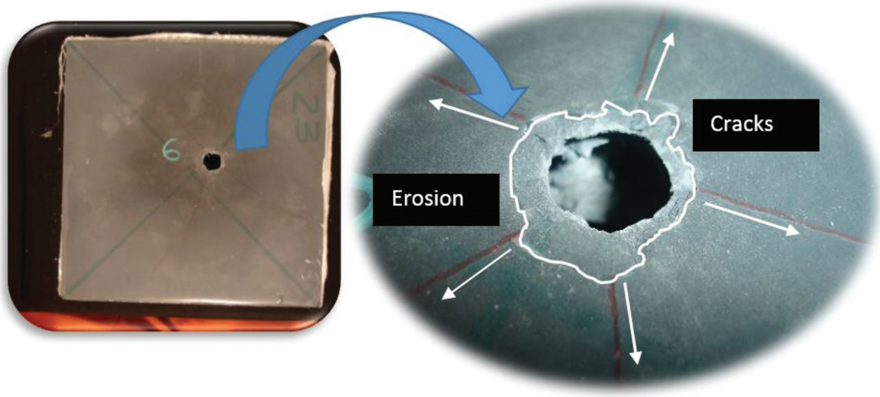

Figure 7. Footprint of the projectile on the ceramic plate.

4.1.1. Fractography of Case I

The footprint of the projectile after passing through the system, the flexible fabric material ultrahigh molecular weight polyethylene, important evidence deformations caused by the moving projectile, and fractures shown are reflected in these images.

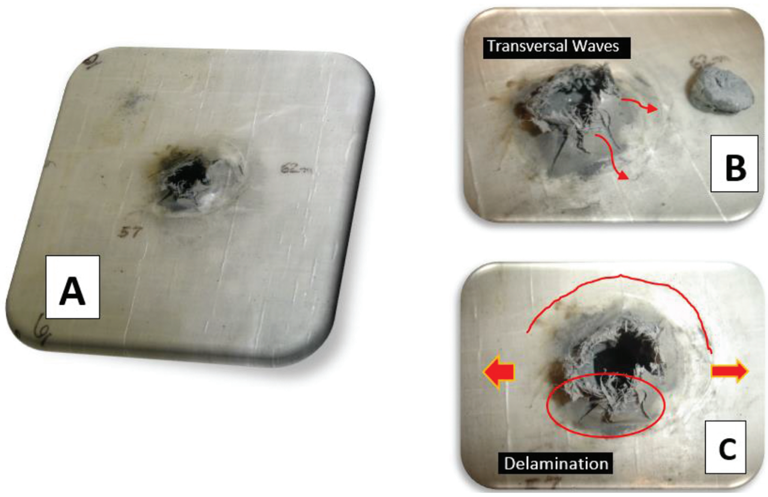

Figure 8. Images to backing fractography.

http://dx.doi.org/10.5772/63576

The isometric view of the composite system is observed in **Figure 8**. The overall damage done by projectile in the material can be seen in image A; an approach breakage of the fibers is shown in image B, along with the tag marked with red arrows in the footprint direction taken by transverse waves, which end with the formation of a neck in the laminate plane (image D), total rupture of the primary fibers that come into direct contact with the projectile, fracturing the flexibility scheme delamination near the area impact. The deformation of the polyethylene layers results in a 12 mm high cone, with almost 40 mm base diameter and 18 mm in the outlet of the projectile; the fiber tear around the hole and image B together with the cone can be seen; deformation caused to the projectile as a result of the penetration process.

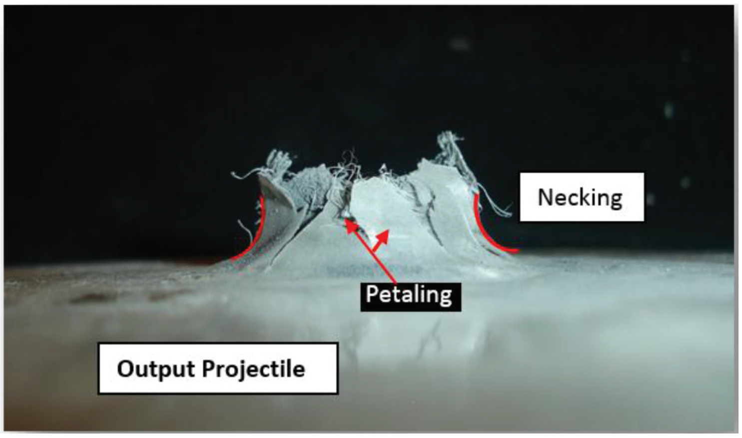

Figure 9. Output of the projectile.

Figure 9 shows the formation of a neck (necking) in the laminate plane, the total disruption of the primary fibers that come into direct contact with the projectile; the projectile completely passes through detailed, they deform the polyethylene layers forming a 12 mm high cone with resulting delamination process with cross section of the projectile on the system; the deformation petals on the flexible layer is called petaling.

4.2. Case II. Flexible fabric in front and ceramic as backing

4.2.1. Fractography of Case II

Figure 10 shows the location of the plates and the direction of impact test that was obtained after subsequent analysis of fractography.

In **Figure 11**, as shown from top to down, the plate is in isometric view, where the penetration hole of the projectile, in image A, shows the detailed view with increased detail in which the crater is formed with broken fibers, the shearing caused tissue and adjacent tissues delamination of the crater. Image B is observed, twisting and fusing the fibers as the result of mechanisms present after impact stress, image C is detailed in the image cutting and twisting the fibers of polyethylene during ductile voltage departure.

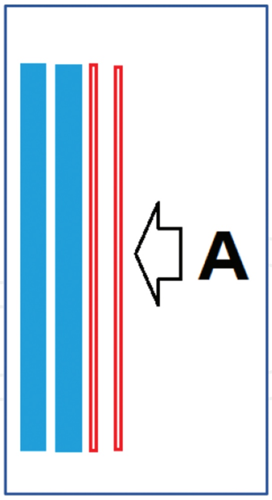

Figure 10. Projectile input direction side A, impact thought UHWMPE.

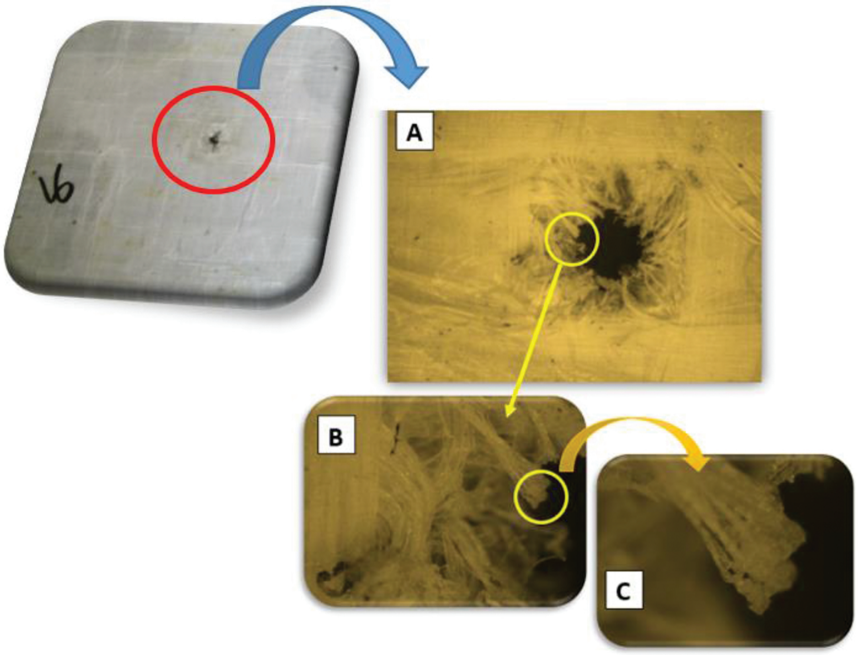

Figure 11. Fractography in the projectile output zone.

In **Figure 12**, the fractography of a system receiving the projectile double ceramic plate that is 10 mm thick and double back sheet flexible polyethylene is shown; image A is highlighted by the mark left by the projectile detailed, which enters flexible face with a hole diameter of the projectile (9 mm), greater penalties, and the rear face forming a crater that is eroded in an inhomogeneous way around the inlet port, cracks occur, which travel only by presenting external ceramic plate breakage. Rupture plates with crater formation in stages with the passage of the projectile are observed. The geometry of the crater [6, 15, 16] has formed in the radial symmetry breaking evenly.

http://dx.doi.org/10.5772/63576

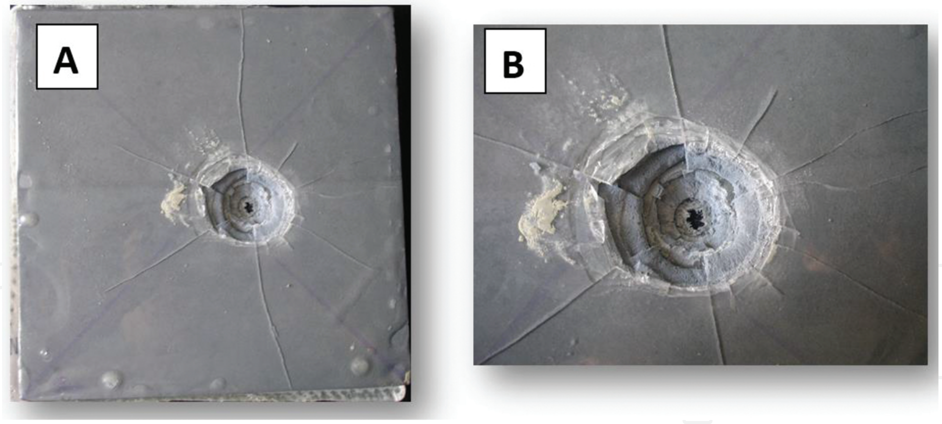

Figure 12. Fractures and cone on the plate "Backing".

In **Figure 13**, a frontal approach presents originated crater, streaking in the resin layer with a radial direction and erosion on the area near the impact surface is highlighted. The strain energy breaks the crater forming cracks from the edge to the back of the panel, which travel through the ceramic material, the breakage of fibers near the orifice, and close to delamination contact area.

Figure 13. Crater originated in the double ceramic plate.

In **Figure 14**, the morphology of the system in cross section cab be observed, which was created using water jet cutting. The image in the input direction of the projectile, which originated a large area delamination and spalling inside the plate, and in the radial direction of the projectile is observed. It is observed that vacuum is created conically. Interlayer resin deformation only in the input diameter of the projectile in the plate target can be seen; it can be ensured that achieving attenuate kinetic energy, which is distributed in the ceramic plates, meaning through spalling, but without stopping the projectile, shows that the resin layer remains intact and shows good adhesion with the ceramic. It can be stated that the ceramic dissipates energy with the formation of the crater, along with the flexible system, which is seriously affected.

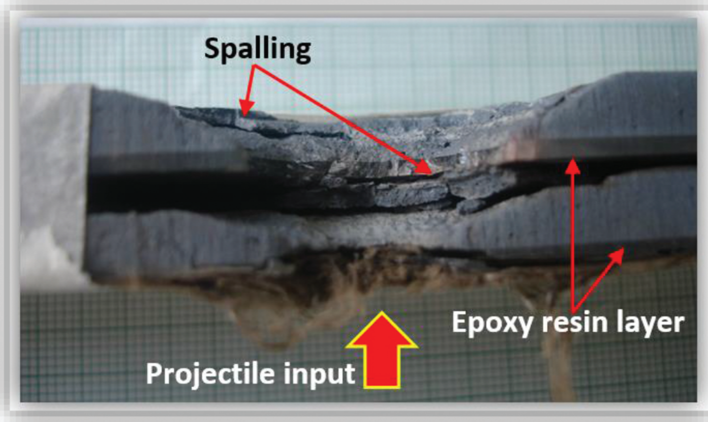

Figure 14. Fractography cross-sectional view.

In **Figure 15**, some failure mechanisms as spalling between the ceramic layers and the resin layer can be seen in cross-section, which can be realized as the intraseparation and interlaminar ceramic where the fracture material arrangement similar to leaves is superimposed without total detachment. Also, the crack initiation deforming plate from contact with the projectile is observed traveling environment symmetrically radial through the complete system. Some fractures travel lengthwise through porosity ceramic into contact with the gaps or vacancies in the resin layer, which ends up slowing the advance of the fracture plate in the bottom plate continuous plastic deformation with continuity conical-shaped crater to the total output of the projectile, with the red arrow penetrating the sense indicated.

A detail of the cross section of image A spalling is illustrated in **Figure 16**, which is mentioned in the previous paragraph describing environment puncture by the displacement of the plates; this dislocation of the solid layers is possibly the result of the trip transverse waves of energy during the compression exerted by the projectile. The eroded layer is the result of pressure and high temperature as a mark left by the passage of the projectile during contact with the ceramic plates. In image B, the detailed projectile outlet and a portion of tissue shearing during impact stress as observed drag is shown.

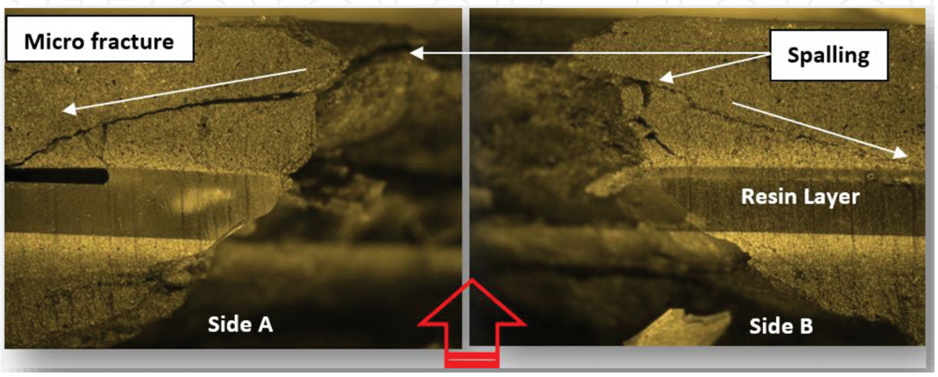

Figure 15. Fractography double cross view on the ceramic plate.

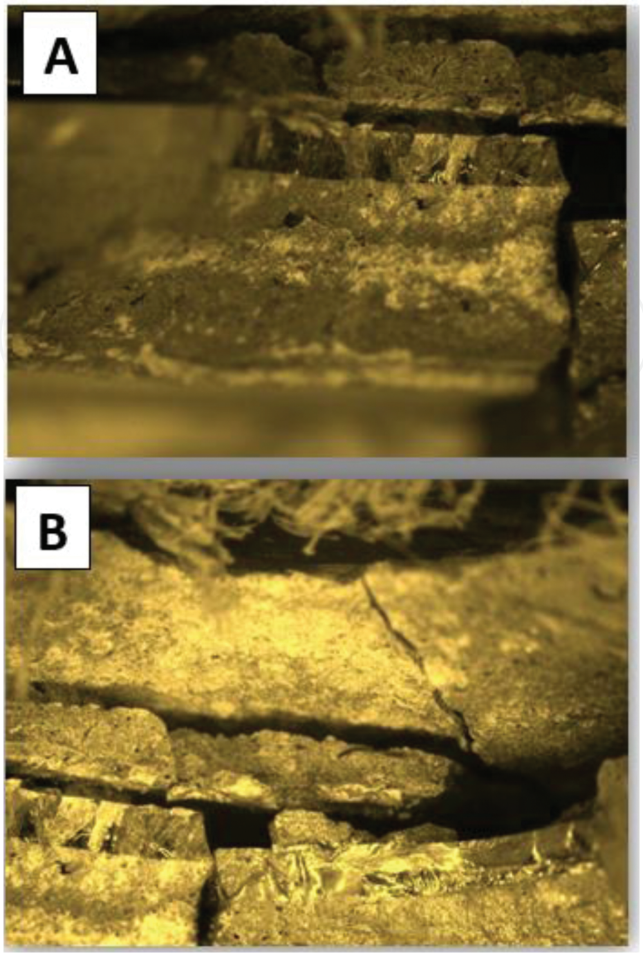

Figure 16. Detail of the passage of the projectile by the ceramic body.

4.3. Fracture mechanisms in the epoxy resin layer

In **Figure 17**, a trace of the passage of the projectile, which crosses the plate, causing a crater with a diameter greater than the projectile penalties, erosion causes environment entry system, leaves a marked trace of the shear wave, is observed as deformation caused by high contact temperature and the velocity of the projectile, which dissipates some of the kinetic energy in the radial cracks from the impact point.

In **Figure 18**, the footprint on the plate epoxy resin is shown in detail in image A, the projectile enters the plate melting the resin perimeter of hole, and waves are formed due to the rapid solidification of the material before the passage of the projectile with high temperature. In image B, the morphology of details of one of the waves and the rough texture caused by the process of rapid cooling of the material is observed. In image B, the crater is observed and chipping caused in the layer of flexible polyethylene is shown, which solidified with resin around the crater erosion caused in response to the opposition of the material passage of the projectile.

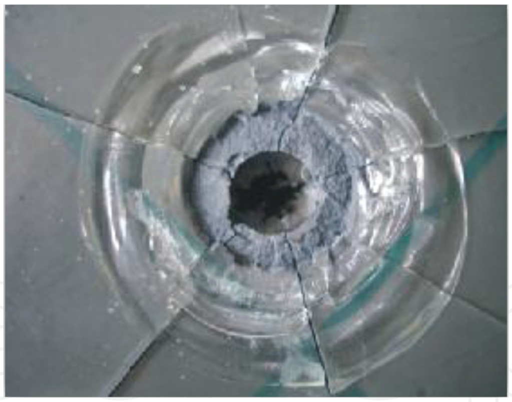

Figure 17. Footprint of the projectile on the layer epoxy resin.

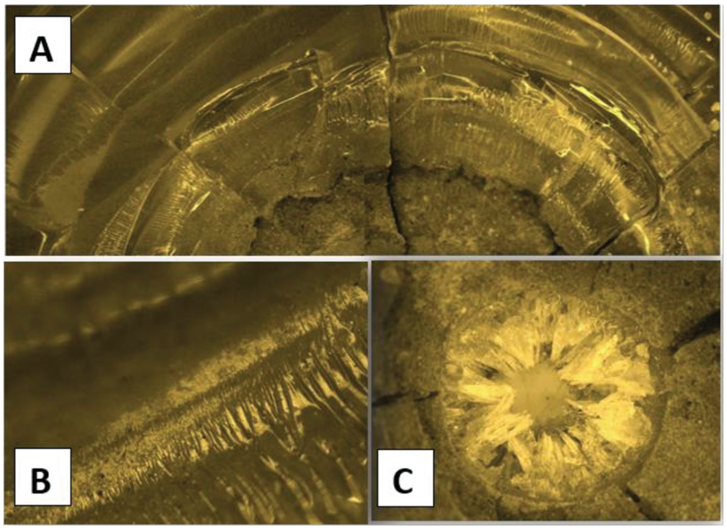

Figure 18. Footprint waves on the layer of the epoxy resin.

4.4. Fracture mechanism in ceramic low-porosity plates in front and UHWMPE as backing

In **Figure 19**, the result of the impact on a plate of silicon carbide with 5% porosity is closely illustrated; it was manufactured by means of high pressure and temperature. In image A, a view of the isometric plate is generally observed, in which in the center the product of impact deformation can be seen, with the distribution transverse cracks the crater. In image B, the front view of the crater on the ceramic plate is observed in the joint caused by shear waves that completely fractured ceramic cracks. In image C, the center of the impact is displayed, which completely distorts the projectile, completely dissipating the kinetic energy, and the fracture was complete. The silicon carbide plate was very efficient, it was observed that totally absorbed kinetic energy of the projectile, the plate with geometric characteristics and low porosity compared to original plates, was used in the exploration, whereas the rear layer of polymeric fabric did not present deformation and remained intact against impact, worked to contain remaining fragments of ceramic originating from direct contact with the projectile.

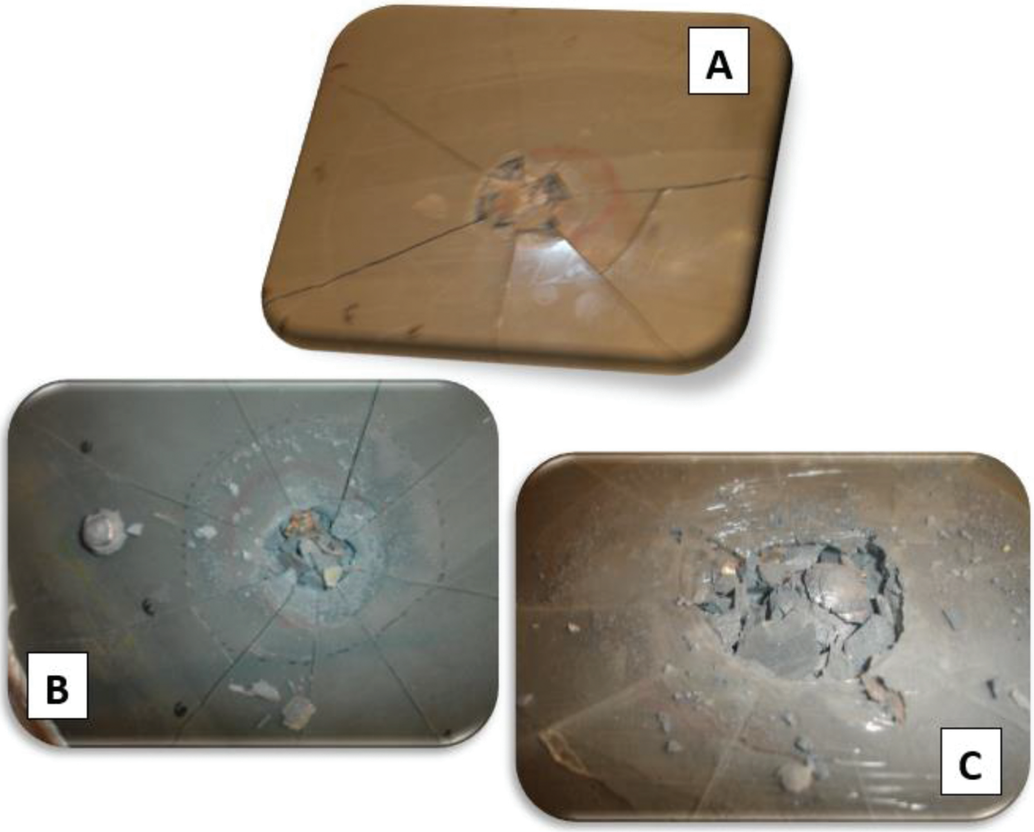

Figure 19. Fractography in the ceramic plate with reduced porosity.

The failure mechanisms generally observed in this exploration have been reported, a brief description of different types of failure is presented below. The formation of a crater followed by crack propagation is reported in the rigid ceramic systems; Horsfalla et al. [17] and Medvedovski et al. [18] found that it was also possible to identify the individual component in a compound system with different functions during the deformation of the panel in these publications and that the form of energy dissipation also depends on the materials and the manufacturing processes. The compaction process and pressing of ceramic powders determine the porosity in the final product, with these processes it seeks to maximize the mechanical protection systems with high-capacity energy dissipation properties, characteristic involves reducing the porosity at least; the pores are small defects that may act as stress concentrators and initiators for material failure [19].

It has been found that the composite systems surpass the dissipation of energy capacity; at the conventional systems used without any combination, Sherman and Brandon [20] detected a sequence in the mechanisms of energy dissipation in a ceramic plate, such as the formation of radial cracks during traction associated with this downward tensile strength of ceramics. Cunniff et al. [21] presented the performance of ballistic polymer fiber; they also identified the mechanisms of fracture in flexible fibers and its potential energy absorption. In the flexible system, another predominant mechanism in tissue polymers during the dissipation of kinetic energy is the formation of a conical pyramid backing material; it was observed that the strain and deformation are function of the distance of the impact; therefore, the wires are closer, experience stress failure, whereas the most distant point of impact wires have no tension [22].

4.5. Kinetic energy dissipation

The basis for the model applied to the evaluation of these analyses was developed by Morye et al., being the most similar characteristics presented for the study [23]. This model analyzes the tensile failure of the primary fibers, elastic deformation of the secondary fibers, delamination, breakage of the system matrix, and the formation and movement, which are five deformation mechanisms that contribute to the dissipation of energy from the projectile and are considered a cone on the rear side of the plate of the composite. The five energy absorption mechanisms that were applied are as follows:

Equation	Application	
$ET = E_{FP} + E_{FS} + E_{KC} + E_{DL} + E_{RM}$	Explained in the previous paragraph	Eq. (1)
$ET = E + W$	E is the difference between the initial and residual kinetic energies, this corresponds to the energy lost by heat and deformation during impact is calculated as follows (Eq. (3))	Eq. (2)
$E = \frac{1}{2}mp(v_s)^2$ $E = \frac{1}{2}mp(v_s)^2 - \left[\frac{mp}{mp+ms}\right]$	V_s is the initial velocity, M_p is the mass of the projectile, and M_s is the plug mass	Eq. (3)
$\frac{1}{2}mp(v_s)^2 + E + W + (mp+ms)Vr^2$	The additional kinetic energy (W) can be lost through deformation during drilling due to the presence of the circumferential cutting zone	Eq. (4)
$E_{kci} = \frac{1}{2}m_{ci}Vi^2$	m_{ci} is the mass of the cone formed on the rear face of the composite plate and is determined by Eq. (5)	Eq. (5)
$m_{ci}Vi^2 = \pi(R_{ci}^2)(e)(\rho)$	ρ is the density of composite laminate, e is the flexible laminate (UHWMPE) thickness	Eq. (6)
$E_{kci} = \frac{1}{2}\pi(R_{ci}^2)(e)(\rho)(v_i^2)$		Eq. (7)
$ET = E + W + Ekci$	Empiric equation used for this exploration	Eq. (8)

Table 1. Equations used in the analysis of kinetic energy dissipation.

The total energy absorbed by the laminate composite in Eq. (1): where EFP is the energy absorbed by the failure of the primary fibers; SAI, energy absorbed by the elastic deformation of the secondary fibers; EKC, energy absorbed in the formation and movement of the cone at the rear face of the panel; EDL, energy absorbed due to delamination of the material; ERM, energy absorbed due to breaking of the matrix.

Another model studied was presented by Retch and Ipson [23, 24]; they presented a semiempirical model where a balance of kinetic energy is analyzed and the energy is dissipated by the generation of the crater during the impact (Eqs. (6) and (7)). For the study of energy, balance takes into account the following characteristics of the composite system: mass, density, and dimensions of the system; mass, diameter, and velocity of the projectile; and residual impact velocity and mass of the plug (product ejected by impact); the energy balance formula is presented in **Table 1**.

FMJ (full metal jacket) round tip 9 mm diameter × 19 mm in length with a nominal mass of 8.0 g and a speed of 436 m/s					**Projectile**
Case study	**Input projectile side**	**Mechanism observed**	**Kinetic energy projectile (J)**	**Kinetic energy dissipated (J)**	**Kinetic energy to retain (J)**
Case A	Double flexible fabric in front and ceramic double plate as backing	Crater formation on ceramic backing, ductile fracture in the fibers, defibrillation	**577.6**	**342**	**237**
Case B	Ceramic double plate in front and double Flexible fabric as backing	Low crater formation on ceramic backing, fracture in he fibers nearly to crater and conic formation on the UHWMPE backing		**437.382**	**140**
Case C	Ceramic plate with less porosity Single in front and double Flexible fabric as backing	Crater formation on the ceramic plate with multiple fracture, neither deformation in the backing face.		**577.6**	**0**

Table 2. Results of kinetic energy dissipated.

The analysis complemented with the study of flexible and rigid systems, abstracted to empirical analysis, modeling the energy absorption by the mechanism of formation of the cone on the rear side of the laminate, whose vertices move at the same speed of the projectile (V_i) and the depth thereof is equal to the total displacement of the projectile (D_i), during contact, therefore the kinetic energy of the cone E_{kci} can be determined using Eq. (6). In this model, a general energy balance where we can analyze the absorption due to the formation of the crater and the mass displaced by the projectile, valuable information for analysis systems in predominantly rigid exploration; this model can be complemented performing the model presented by Morye et al. with Eqs. (6) and (7), assuming that the flexible polyethylene backing (UHWMPE) remains bonded to the ceramic and can be analyzed as a circular membrane with an initial mass that is produced in the system by reducing the velocity of the projectile. From Eqs. (5) to (7), the kinetic energy is obtained due to the formation and movement of the cone on the rear side of the composite plate. The results are shown in **Table 2**.

5. Conclusions

The fractography found in the ceramic component is defined in the formation of a crater, erosion, and fracture, while the polymer components were observed as mechanisms for energy dissipation, delamination, cone formation, petals, breakage, and melting fibers.

A large number of failure mechanisms were observed in the design sandwich double ceramic plate in the front and double sheet of UHWMPE in the back; they were observed as dissipation mechanism energy, fragmentation and erosion on ceramic plates, forming petals, delamination and cuts in polymer sheets; these evidences in the photographs were indispensable data for the analysis of kinetic energy dissipation using the semiempirical models of Reich and Ipson and Morye et al.

In this exploration, it was possible to observe the influence of the manufacturing process in a system of high requirements in terms of dissipation of kinetic energy, which is why the analyzed total dissipation of energy system was obtained by high pressure and high temperature of case C as compared to cases B and C, which were manufactured by traditional techniques.

Acknowledgements

The authors specially thank to Knight Group Owners Caballero SAS International, headed by the CEO engineer Miguel Caballero, for their decisive collaboration, disposition, and financing of ballistics tests, laboratories and polymeric material. They also thank the company Quimiresinas for its contribution in the epoxy resin and to the Universidad Nacional de Colombia, Medellin, at the laboratory metallography and materials testing by providing resources for the acquisition of most of ceramic plates used in this exploration. Acknowledgments in memory to Military Engineer Edgar Caicedo for was showing me the way of success in the Engineering Design.

Author details

Giovanni Barrera Torres[1*], Juan Manuel Vélez[2] and Carlos Mario Gutierrez[1]

*Address all correspondence to: gbarrerat01@gmail.com; giovannibarrera@itm.edu.co

1 Metropolitan Institute of Technology (ITM), Medellin, Colombia

2 National University of Colombia, Medellin, Colombia

http://dx.doi.org/10.5772/63576

References

[1] H. Harel, G. Marom. Delamination Controlled Ballistic Resistance of Polyethylene/ Polyethylene Composite Materials. Jerusalem, Israel/52526 Ramat Gan, Israel: Casali Institute of Applied Chemistry, The Hebrew University of Jerusalem/S. Kenig Department of Plastics Engineering, Shenkar College. 2000.

[2] A. Bhatnagar. Lightweight Ballistic Composites, Military and Law-Enforcement Applications. Cambridge, England: Woodhead (Woodhead Publishing and Maney Publishing on behalf of The Institute of Materials, Minerals & Mining). pp. 4–7. 2006.

[3] George Murray, Charles V. White, Wolfgang Weise. Introduction to Engineering Materials. Chapter 1, Classification of materials. 2nd ed. Taylor and Francis Group. pp 13–15. 2008.

[4] Donald R. Askeland, Pradeep P. Phulé, "Wendelin J. Wright. Composites:TeamWork and Synergy in Materials". *The Science and Engineering of Materials* , Stamford, Cengage Learning, pp. 653–687. 2006.

[5] S.K. McGuire, M.G. Jenkins. Ceramics Testing. Stanford, California/Seattle, Washington: Stanford University/University of Washington, Chapter 23. 2007.

[6] F.G. Díaz–Rubio. Mechanical Characterization of Advanced Ceramic Materials at High Strain Rates; Doctoral Thesis, Aeronautical Engineering. pp. 13,15. 1999.

[7] James K. Wessel. Advanced Ceramics materials. Handbook of Advanced Materials: Enabling New Designs. John Wiley & Sons, Inc. pp 65–88. 2004.

[8] Eugene Medvedovski. Ballistic performance of armour ceramics: influence of design and structure. Part 2. Ceramics International 36 (7).pp 2117–2127. 2010.

[9] P. Colombo, F. Zordan, E. Medvedovski. Ceramic–Polymer Composites for Ballistic protection. Padova, Italy: Dipartimento Di Ingegneria Meccanica, Settore Materiali Università Di Padova Via Marzolo. 2005.

[10] F. Vargas, E. López, D. López, J. Areiza, M. Monsalve. Manufacture of Silicon Carbide Tubes for use as Heating in Ovens and Heating Systems Body. Group Pyrometallurgical and Materials research, Universidad de Antioquia. 2008.

[11] R. Obeso Cobo and F.G. Díaz–Rubio. Dynamic properties study of ceramics materials. Application Al– SiC. Canales y Puertos. Madrid: Department of Materials Science. pp 12, 13, 45–,46. 2004.

[12] S.K. Garcia Castillo. Analysis of Laminated Composite Materials in its Plane and Preload Subjected to Impact University Carlos III of Madrid. Department of Continuum Mechanics and Structural Analysis Doctoral Thesis. pp. 12,14. 2007.

[13] F.L. Matthews and R.D. Rawlings. Composite Materials, Engineering and Science. Woodhead Publishing. pp 173, 372, 373. 1994.

[14] Ballistic Resistance of Body Armor, NIJ Standard–0101.06. National Institute of Standards and Technology Prepared For: National Institute of Justice. Washington, DC. July 2008. http://nist.gov/oles/upload/ballistic.pdf.

[15] D. Sherman, D.G. Brandon. The ballistic failure mechanisms and sequence in semi-infinite supported alumina tiles. Journal of Materials Research. 12:1335–1343. 1997.

[16] Zukas, Jonas A., Nicholas, Theodore, Swift, Hallock F., Greszczuk, Longin B., Curran, Donald R. Impact Dynamics. Wiley. 1982.

[17] I. Horsfall, S.J. Austin, W. Bishop. Structural ballistic armour for transport aircraft. Materials & Design, 21(1):19–25. 1999.

[18] H.L. Gower, D.S. Cronin, A. Plumtree. Ballistic Impact Response of Laminated Composite Panels. International Journal of Impact Engineering pp.1000–1008. 2007.

[19] V.A. Greenhut. Characterization of ceramics and glasses: an overview. Engineered Materials Handbook, Ceramic and Glasses. Vol. 4, ASM International. 1991.

[20] Dov Sherman and D.G. Brandon. Supported Alumina Tiles. Journal of Materials Research. V.12. pp 1335–1343. 1997.

[21] P.M. Cunniff, M.A. Auerbach. High performance "m5" ballistic fiber.http://web.mit.edu/course/3/3.91/OldFiles/www/slides/cunniff.pdf. April 04.2016.

[22] A. Bhatnagar. Lightweight Ballistic Composites, Military and Law-Enforcement Applications. Cambridge, England: Woodhead (Woodhead Publishing and Maney Publishing on behalf of the Institute of Materials, Minerals & Mining). Chapter 28, pp 222–223. 2006.

[23] S.K. Garcia Castillo. Análisis de laminados de materiales compuestos con precarga en su plano y Sometidos a Impacto Universidad: Carlos III de Madrid. Tesis Doctoral Año. pp 124–139. 2007.

[24] Ashok Bhatnagar. Lightweight Ballistic Composites: Military and Law-Enforcement Applications. CRC Press (Woodhead Publishing and Maney Publishing on behalf of the Institute of Materials, Minerals & Mining). Chapter 28. pp. 229,230. 2004.